Nearly golden-ratio order in Ta metallic glass*

Yuan-Qi Jiang(蒋元祺)[1,2,†] and Ping Peng(彭平)[3]

[1] *Department of Physics, Nanchang Normal University, Nanchang* 330032, *China*
[2] *College of Physics, Jilin University, Changchun* 130012, *China*
[3] *School of Material Science & Engineering, Hunan University, Changsha* 410082, *China*

(Received 28 November 2019; revised manuscript received 10 February 2020; accepted manuscript online 18 February 2020)

The formation of mono-atomic tantalum (Ta) metallic glass (MG) through ultrafast liquid cooling is investigated by *ab-initio* molecular dynamics (MD) simulations. It is found that there exists nearly golden ratio order (NGRO) between the nearest and second nearest atoms in Ta MG, which has been indirectly confirmed by Khmich *et al.* and Liang *et al.*. The NGRO is another universal structural feature in metallic glass besides the local five-fold symmetry (LFFS). Further analyzing of electronic structure shows that the obvious orientation of covalent bond could be attributed to the NGRO in amorphous Ta at 300 K.

Keywords: nearly golden ratio order (NGRO), metallic glass, tantalum, *ab-initio* molecular dynamics (MD) simulation

PACS: 61.25.Mv, 64.60.Cn **DOI:** 10.1088/1674-1056/ab773f

1. Introduction

Since the first discovery of metallic glass (MG) in the 1960s,[1] understanding the local atomic structures of various types of MGs has never stopped and still remains a crucial issue in materials science.[2–4] Many researchers have recognized that icosahedral clusters play a key role in the glass formation of transition metals–transition metals (TM–TM) amorphous alloys.[4–6] In the literature, one can easily find several studies that are carried out using molecular dynamics (MD) simulations which show that these icosahedral clusters not only impact on the thermo-dynamical properties of metal and alloy melts,[7–15] but also exhibit excellent structural stability[13,14] and configuration heredity during the rapid solidification.[4,16] Merely, difference of atomic size and various chemical ordering arrangements of amorphous alloys are not ignored due to their multi-component chemical nature.[7] Therefore, it is highly desirable to carry out a specialized investigation on the local atomic structures of the pure mono-atomic metallic glass to shed more light on the atomic size and arrangements of various chemical orderings.[7,17] Recently, by combining *in-situ* transmission electron microscopy observation and atoms-to-continuum modeling, several pure refractory body-centered cubic (BCC) metals, such as liquid Ta, V, W, and Mo, were successfully vitrified to form metallic glasses by achieving an unprecedentedly high liquid-quenching rate of 10^{14} K/s.[18] The ingenious experiment filled part of the gaps between experiment and simulation,[17] and paved the way for investigating the essential structural characteristic of metallic glasses by computer simulation. Namely, not only the cooling rate used in the experiment is rapid enough to be within the computing capability, but also the mono-atomic amorphous metals are an ideal model to understand the atomic structure of metallic glass.[17,18] Following the experiment,[18] series of quenching melts of pure refractory BCC metals were simulated by *ab-initio* MD[19] and classical MD[17,20] methods. For example, Zhang *et al.*,[19] Khmich *et al.*,[20] and Jiang *et al.*[13] investigated the local atomic structure,[11] glass formation,[20] and cluster evolution[21,22] in the rapidly solidified mono-atomic metallic liquid Ta, respectively. And they spontaneously pointed out that the dominant Voronoi polyhedral in Ta mono-atomic MG is the distorted icosahedra rather than the perfect icosahedra.[20] Khmich *et al.*[20] obtained the ratio R_i/R_1 of radial distribution function (RDF) and showed the presence of a hidden crystalline order in Ta mono-atomic MG. Wu *et al.*[17] found that the local topologically close-packed (TCP) structures are commonly seen for the liquid and amorphous Ta.[17] Yang *et al.* further reported a fractal characteristic in the quenched Ta.[22] Gangopadhyay *et al.* predicted T_g for many elemental metals from thermo-physical properties of liquids[23] and so on. Obviously, although the unique internal structure of MG underlies their interesting properties, but fundamental knowledge on the atomic structure aspect of MG remains as opinions vary, no unanimous conclusions can be drawn.

Based on the above reason, the formation of mono-atomic Ta MG through ultrafast liquid cooling is investigated by *ab-initio* MD simulation. It is found that not only icosahedral short-range orders (ISROs) and icosahedral medium-range or-

*Project supported by Qinglan Scholars Program of Nanchang Normal University and Natural Science Foundation (Grant No. 20171BAB216001), Scientific Research Project of Education Department of Jiangxi Province, China (Grant Nos. GJJ191114, GJJ161242, and GJJ171110), and the National Natural Science Foundation of China (Grant No. 51871096).

†Corresponding author. E-mail: yuanqi325@163.com

ders (IMROs) coexist in the Ta metallic glass, but also more importantly there exists a nearly golden ratio order (NGRO) in the mono-atomic Ta MG. And we deduce that the NGRO is another universal structural feature in metallic glass besides the local five-fold symmetry (LFFS). To the best our knowledge, the NGRO in mono-atomic Ta MG is the first time reported up to now.

2. Computational method

The simulation in the present work was conducted by employing the Vienna *ab-initio* simulation package (VASP)[24,25] with the generalized gradient approximation[26] for the exchange correlation functional and the projector augmented wave[27] method for the electron–ion interaction. The Newton's equation of motion was solved via the Verlet's algorithm with a time step of 5 fs and the simulation was performed at a normal precision. The wave functions were sampled on $1\times1\times1$ k-point mesh in terms of the Monkhorst–Pack scheme.[28] The plane wave cutoff energy is 280 eV, and the energy convergence criterion of electronic self-consistency is chosen as 1.0×10^{-4} meV/atom for all the calculations. Then, *ab-initio* MD simulations of the rapidly solidified process of liquid metal Ta were carried out, in which 108 atoms in a cubic box (11.5 Å×11.5 Å×11.5 Å) subjected to the periodic boundary condition were considered. The metal Ta was initially melted and equilibrated for 10 ps at 4000 K well above the experimental melting temperature $T_{\rm m}=3290$ K,[20] next the 108 Ta atoms were rapidly cooled down from 4000 K to 300 K with a cooling rate of 5×10^{13} K/s. Three reference configurations (108 atoms in each configuration) of Ta were used in the potential fitting process and the valence electron configuration of Ta in the density functional theory calculation is $5d^36s^2$. At each temperature, the ions were systematically varied through the relaxation in VASP and a parallel implementation of the RMM–DIIS (residual minimization method and the direct inversion in the iterative subspace) method with respect to each band in this paper.

In addition, we have further calculated the density of the 108-Ta system by Large-scale Atomic/Molecular Massively Parallel Simulator (LAMMPS)[29] for comparing the behaviors of the rapid solidified processes, which is plotted in Fig. 1(b). Their motion equations were solved by Verlet's algorithm in the velocity form with a time step of 1 fs. Constant pressure p and temperature T were imposed by a modified Nose–Hoover method[30] for both p and T variables and an embedded-atom model (EAM) potential[31] was utilized. The silver was initially melted and equilibrated for 10 ns at 4000 K well above the experiment melting temperature $T_{\rm m}=3290$ K,[20] and subsequently the liquid was cooled down to 300 K at the same cooling rate of 5×10^{13} K/s. The cooling run was performed in the *NPT* ensemble with zero pressure.

3. Simulation results

3.1. Systemic total energy and density

Before analyzing the microstructures of the system in detail, the evolution of the systemic total energy per atom (E) of the 108-Ta system as a function of temperature during cooling is firstly analyzed for three kinds of initial configurations, as illustrated in Fig. 1(a) together with a snapshot of the system at 300 K. From Fig. 1(a), one can see that the curves of energy fluctuate very obviously at high temperatures, then the different energy curves converge to be consistent at temperatures below about 1750 K. Upon further cooling from 1750 K to 300 K, E changes smoothly, the oscillatory extent becomes weaker, and gradually E exhibits a linear dependence of temperature. Hence the apparent glass transition (GT) temperature ($T_{\rm g1}$) is determined to be about 1750 K by extrapolating the line of the E curves from 300 K to 1750 K. The $T_{\rm g1}=1750$ K is not so far from the experimental value of 1650 K measured by Zhong *et al.*[18] in 2014.

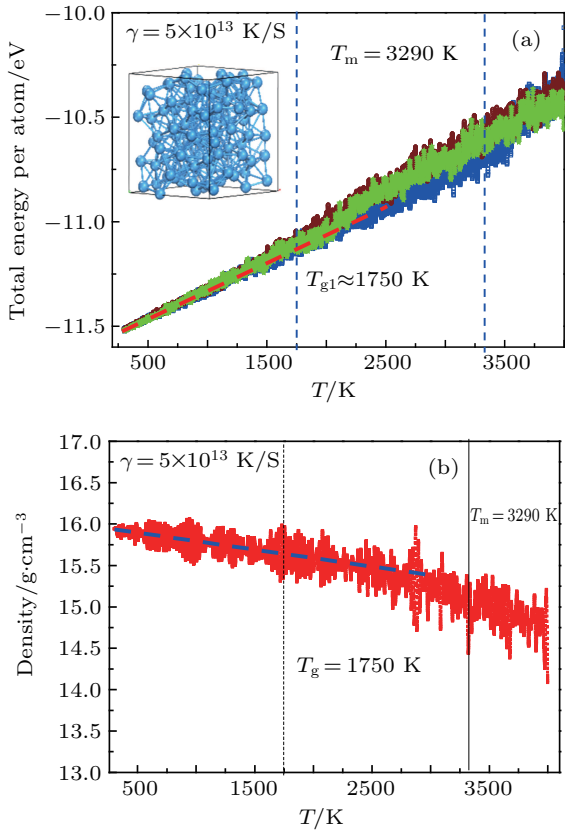

Fig. 1. The temperature T dependence of (a) systemic total energy per atom and (b) density in the rapid solidification.

The atomic packing density is another key feature of the metallic liquid besides the energy. From Fig. 1(b), one can see that the density gradually increases by about 10% from 4000 K to 300 K, indicating that the local atomic arrangements of the

Ta metallic glass must be well correlated and exhibit certain degree of short-range order (SRO) and medium-range order (MRO).[4] In other words, the nearest-neighbor atoms cannot be truly randomly arranged, instead, they must be ordered in some way and to some extent,[4] which are indeed further confirmed by subsequent microstructure analysis in Figs. 2 and 3.

3.2. Radical distribution function and microstructure analysis

The radial distribution function, $g(r)$, also called the pair distribution function or pair correlation function, represents the probability of finding atoms as a function of distance r from an average center atom (Fig. 2(a)).[32] The distribution of interatomic distances, the shell-like structure in the radial direction, and its fading out with increasing distance can be clearly seen in the $g(r)$ of a liquid/glass.[4] In a monoatomic system, we have $g(r) = \frac{1}{4\pi r^2 \rho N} \sum_{i=1}^{N} \sum_{j=1, j\neq i}^{N} \delta(r - |r_{ij}|)$, where ρ is the number density of atoms in the system of N atoms, and r_{ij} is the interatomic distance between atom i and atom j. The $g(r)$ has been widely used to describe the structural characteristics of liquid and solid alloys.[4,33] The variation of the $g(r)$ curves of Ta in the temperature range from 4000 K to 300 K is shown in Fig. 2(b). From Fig. 2(b), one can see that all $g(r)$ exhibits the typical features of either liquid or glass, where a periodically translational long range order is absent. And the first peak of $g(r)$ becomes sharper with the decrease of temperature, indicating that some SRO structures emerge in the system.[2–5,8,34]

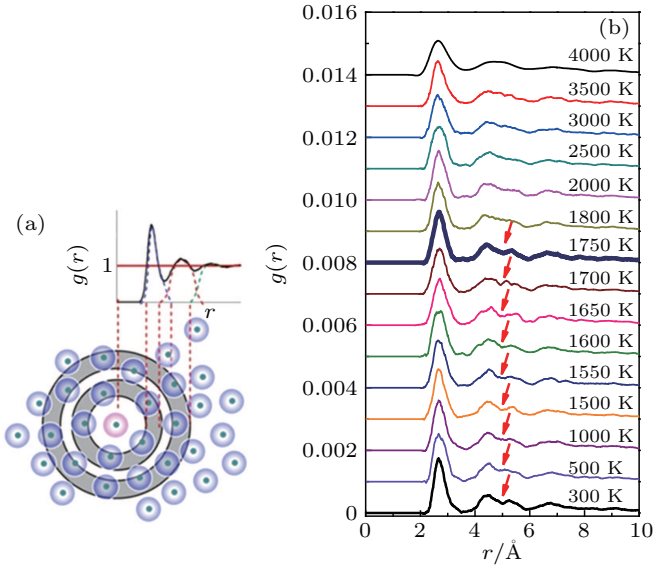

Fig. 2. (a) Schematic diagram of correlation between radial distribution function $g(r)$ and radial distance r.[32] (b) The $g(r)$ of liquid Ta during the rapid solidification at selected temperatures. For guides to the eyes, the splitting position of the second peak of $g(r)$ is marked by red arrow.

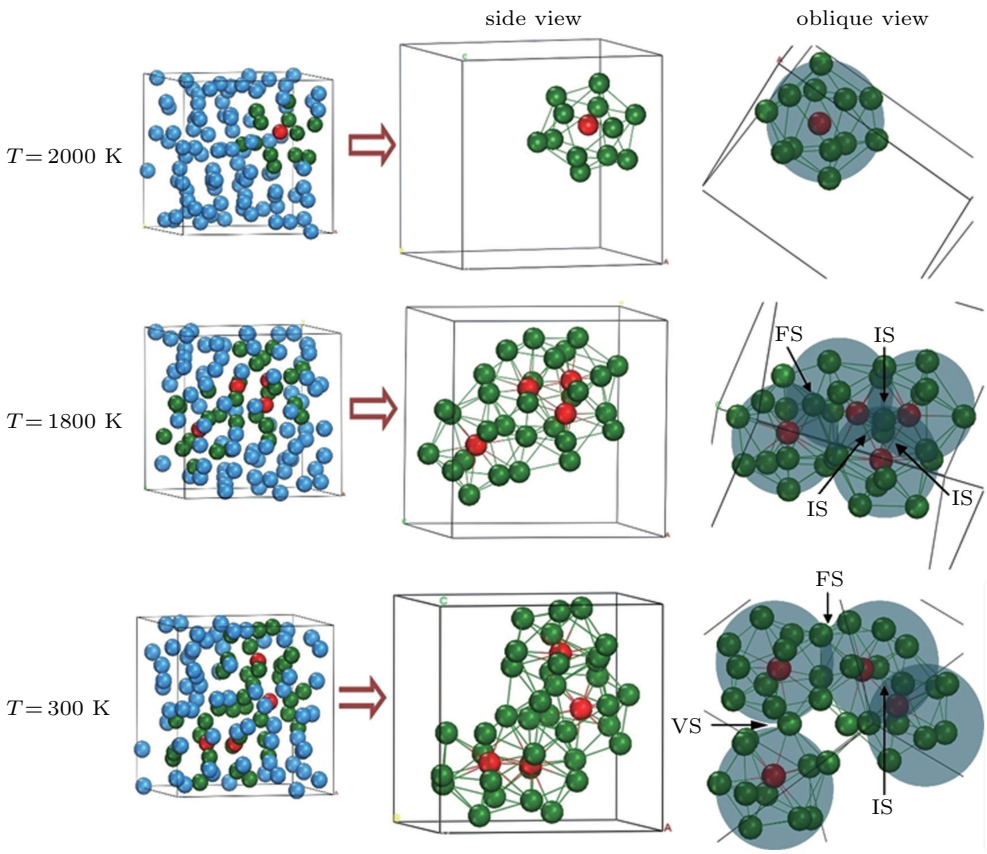

Fig. 3. Schematic diagram of a typical growth of icosahedra clusters in the rapid solidification of Ta metal. The red and green balls denote central and shell atoms of icosahedral clusters. The blue balls denote residual atoms in other local atomic configurations without the tracked icosahedra. The transparent grey roundels denote icosahedral clusters.

More importantly, the split of the second peak of the $g(r)$ curve is usually regarded as a common feature to distinguish glasses from liquids.[33] The splitting positions of the second peak of $g(r)$ are marked by red arrows in Fig. 2(b). From Fig. 2(b), one can see that the split of the second peak of $g(r)$ starts at about 1750 K and becomes more and more pronounced upon subsequent cooling, in which an increasing shoulder further indicates the increase of IMROs with the temperature decreasing. To understand the formation of icosahedra and IMROs during the rapid solidification of the Ta system, the schematic diagram of a typical growth of icosahedra clusters is illustrated in Fig. 3. From Fig. 3, one can see that icosahedra appear at about $T = 2000$ K for the first time, and then quickly expand into IMROs by intercross-sharing (IS), face-sharing (FS), and vertex-sharing (VS) linkages with the decrease of temperature. When the temperature keeps on decreasing to 300 K, figure 3 reveals that the Ta system exhibits an icosahedral saturation state compared to the number of icosahedra at $T = 1800$ K. And the formation temperature (1800 K) of IMROs by IS and FS linkages is approximately consistent with the starting split temperature ($T_{g1} = 1750$ K) of the second peak of $g(r)$ in Fig. 2. It is believed that such splitting arises from the formation of icosahedral clusters in the super-cooled liquids and the rapidly solidified solid is of amorphous characteristics.[34]

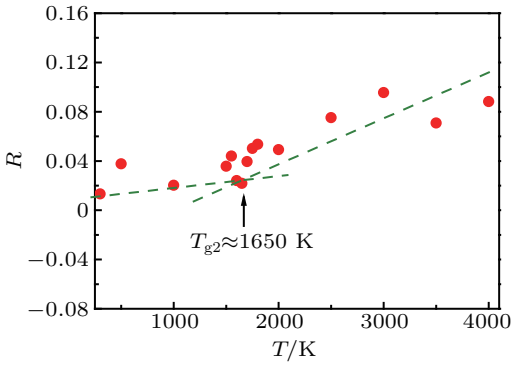

Fig. 4. The ratio of the first minimum to the first maximum of $g(r)$ as a function of temperature T.

In fact, the $g(r)$ curves are used not only to describe the structural characteristics of liquid and amorphous alloys, but also to determinate the GT region from the empirical criterion.[35] As early as in 1978, Wendt and Abraham proposed an empirical criterion using $g(r)$ for specifying the super-cooled liquid/amorphous phase boundary.[35] They defined an empirical parameter $R = g_{min}/g_{max}$, where g_{min} and g_{max} are the magnitudes of the first minimum and the first maximum of $g(r)$, respectively. The empirical parameter R is plotted versus the sequence of temperature in Fig. 4. From Fig. 4, an apparent GT temperature T_{g2} is determined to be 1650 K by extrapolating and intersecting the two linear parts of the R vs. T curve from 300 K to 4000 K. It is noticed that the present $T_{g2} = 1650$ K is lower than $T_{g1} = 1750$ K in Fig. 1, but consistent well with the estimated experimental value of 1650 K in Ref. [18]. Undoubtedly, this empirical parameter R is highly effective for specifying the super-cooled liquid/amorphous phase boundary.

3.3. NGRO in Ta metallic glass

Although LFFS in the form of metallic glasses is considered as the populous structural unit,[4] more universal structural features about NGRO are proposed for the Ta metallic glass in this paper. If a line is divided into two parts, and the ratio of smaller part and longer part is equal to the ratio of longer part and whole length, then the ratio is the idea golden ratio. That is to say, the divided point of the line should be located at 0.618033988749894848$\cdots$ from the mathematics points of view, the digits after decimal in the golden ratio just keep on going and never end. When the ratio is used in cubic geometry, it is called the golden ratio. The standard golden triangle *ABC*, golden rectangle *ABED*, and golden regular pentagon *HGFED* are plotted in Fig. 5, which are extracted from perfect icosahedra with I_h point group symmetry. In Fig. 5, the distances of the nearest neighbor atoms (i.e., $L_{HG} = L_{GF} = L_{FE} = L_{ED} = L_{DH} = L_{AB}$) have to be equal because we have set the distances of the second nearest neighbor

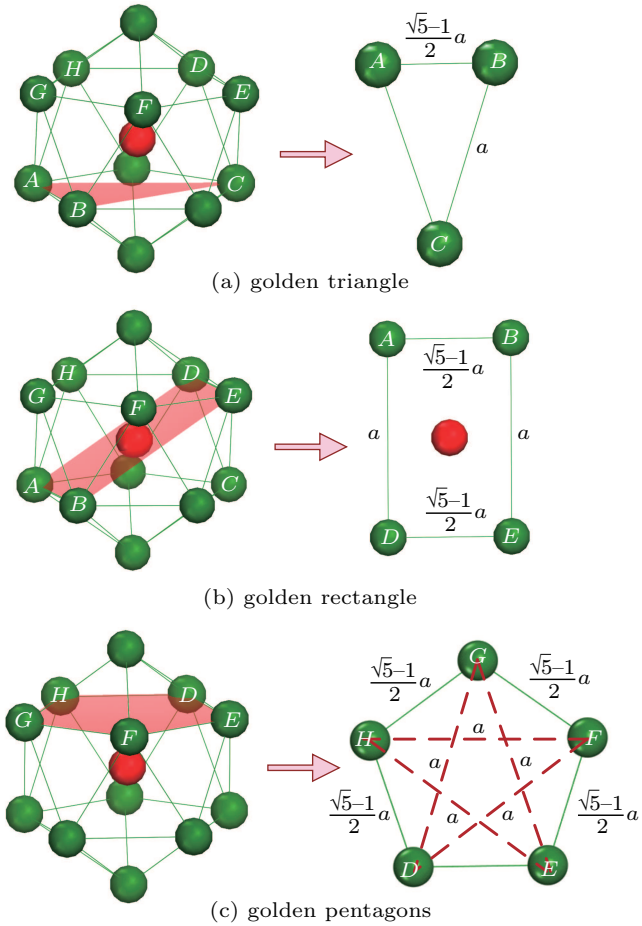

Fig. 5. Schematic diagram of standard (a) golden triangle,(b) golden rectangle, and (c) golden regular pentagon. The red and green balls denote central and shell atoms of icosahedra clusters.

atoms of the icosahedra to be a, i.e., $L_{DG} = L_{DF} = L_{HE} = L_{HF} = L_{GE} = L_{AD} = L_{BE} = L_{AC} = L_{BC} = a$. The mathematic correlative can be attributed to the natural property of icosahedra with I_h point group symmetry. Although such perfect icosahedra do not really exist in liquid and Ta metallic glass owing to the thermal fluctuations,[4] as an idea geometric model, it is very beneficial to explain the originate of NGRO in Ta metallic glass.

In view of the above reasons, the schematic diagram of nearly golden rectangle *IJKL*, golden triangle *RST*, and golden regular pentagon *MNOPQ* in Ta metallic glass at $T = 300$ K are plotted from different angles of view in Fig. 6.

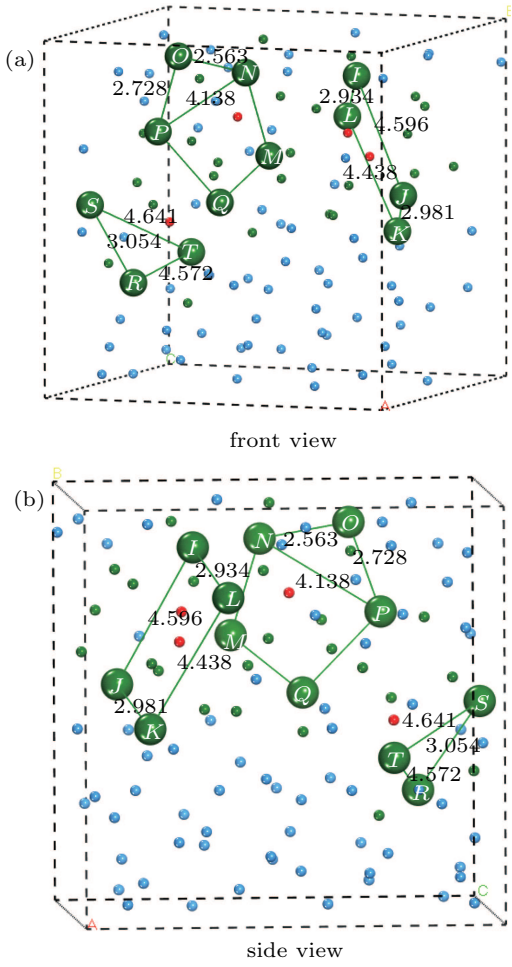

Fig. 6. Diagram of golden rectangle (*IJKL*), triangle (*RST*), and regular pentagon (*MNOPQ*) in Ta metallic glass at $T = 300$ K. The red balls and green balls denote central and shell atoms of icosahedral clusters, respectively. The blue balls denote residual atoms in other local atomic configurations: (a) front view and (b) side view.

From Fig. 6, one can see clearly that the L_{IL} and L_{JK} of rectangle *IJKL* are 2.934 Å and 2.981 Å, respectively. The L_{IJ} and L_{LK} of rectangle *IJKL* are 4.596 Å and 4.438 Å, respectively. So the ratios of L_{IL}/L_{IJ} and L_{JK}/L_{LK} are equal to 0.638 and 0.672, respectively. For triangle *RST*, the ratio of L_{RS}/L_{TS} is 0.658. Meanwhile, the ratio of L_{NO}/L_{NP} for pentagon *MNOPQ* is 0.619. Although the triangle *RST*, rectangle *IJKL*, and pentagon *MNOPQ* are selected randomly from the Ta metallic glass, it is still found that these ratios of distances between the nearest and second-nearest atoms are very close to golden ratio 0.618, especially the ratio of $L_{NO}/L_{NP} = 0.619$ for pentagon *MNOPQ*. So the real secret and hidden information about atomic arrangement in Ta metallic glass will be further analyzed by means of the probability density function (PDF) of atomic distance in the next section.

The PDF is a statistical expression that defines a probability distribution for a continuous random variable as opposed to a discrete random variable. When the PDF is graphically portrayed, the area under the curve will indicate the interval in which the variable will fall. The total area in this interval of the graph equals the probability of a continuous random variable occurring. As an illustrated example, the distributions of probability density (P) as a function of the nearest and second-nearest atomic distances of the Ta system at 3500 K are plotted in Fig. 7. In Fig. 7(a), the green solid and red dash dot lines denote the original P and automatic smoothed P (*SP*, bin size = 0.01 Å, number of bins = 311), respectively. Compared to the green curve with intensive background noise, the automatic smoothed red dash dot line seems more intuited and more beneficial to analyze the results. Thus figure 7(b) only shows the area surrounded by the smoothed *SP* line with x axis, which is divided into two major regions by P approaching to 0. From Fig. 7(b), one can see that the values of green region P_1 and pink region P_2 are 0.3715 and 0.6280, respectively, which denote the integrate of probability density of all the nearest (like L_{IL} and L_{JK} in Fig. 6) and second-nearest (like L_{IJ} and L_{LK} in Fig. 6) atomic distances in the Ta system at $T = 3500$ K, respectively. Herein P_1 is the integrate originated from all the nearest neighbor atomic distances like $L_{HG}, L_{GF}, L_{FE}, L_{ED}, L_{DH}$, and L_{AB} in Fig. 5, and similarly L_{MN}, L_{NO}, L_{LI}, ..., in Fig. 6. Likewise, P_2 should correspond to the integrate of probability density of the second nearest neighbor atomic distances like $L_{DG}, L_{DF}, L_{HE}, L_{HF}, L_{GE}, L_{AD}, L_{BE}, L_{AC}$, and L_{BC} in Fig. 5, and similarly L_{NP}, L_{RT}, L_{ST}, L_{IJ}, and L_{LK} in Fig. 6. Moreover, the ratio of P_1/P_2 is equal to 0.591 from Fig. 7. Based on this, by adopting the exactly identical analysis and characterize method, we have further calculated P_1, P_2 and the ratio of P_1/P_2 from 4000 K to 300 K by interval 50 K for the ultrafast liquid quenching Ta system as shown in Fig. 8. From Fig. 8, one can see that all of P_1, P_2, and P_1/P_2 exhibit random bouncing up and down in the liquid region from 4000 K to 3290 K. Then the P_1 and P_1/P_2 slightly descend and P_2 slightly ascends with decreasing T in the super-cooled liquid region ($T_m \sim T_g$). But an opposing variation tendency is presented when the temperature is below $T_g = 1750$ K. Namely, the lower the temperature is, the integrate value P_1 is closer to 0.382, and both P_2 and P_1/P_2 are closer to 0.618, especially at $T = 300$ K. It is well known that 0.618 be used as the golden ratio in the

mathematic field. So all the values of P_1, P_2, and P_1/P_2 have indicated that the atomic arrangement should be subordinated to nearly golden ratio in the Ta metallic glass. Thus, we define this nearly golden ratio between the nearest and second-nearest atomic distances in the Ta metallic glass as the nearly golden ratio order (NGRO) in this paper.

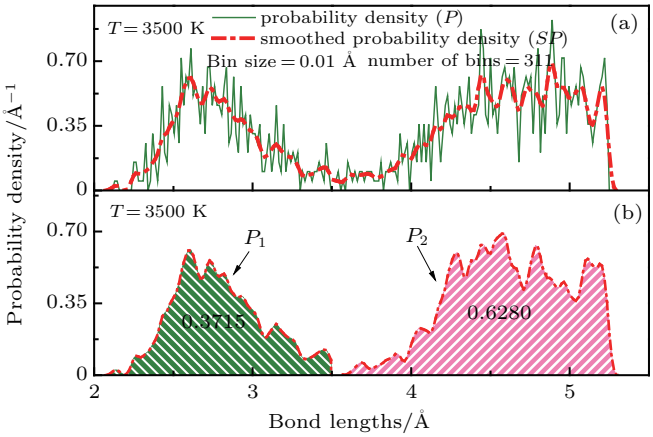

Fig. 7. Distribution diagram of probability density function of bond lengths at $T = 3500$ K.

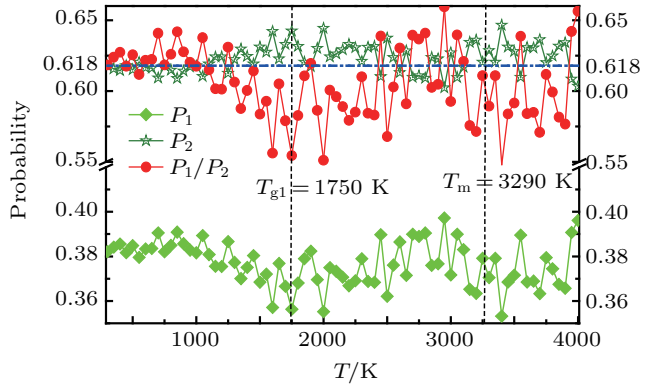

Fig. 8. The temperature T dependence of probabilities P_1, P_2 and the ratio of P_1/P_2 in the rapid solidification of Ta.

While review Fig. 5 again, we have already recognized the golden ratio undoubtedly hidden in the gold rectangle, triangle, pentagon, and so on. And the LFFS has been found to be ubiquitous in liquids and MG.[4,36] That is to say, once we admit that the LFFS is ubiquitous in super-cooled liquids and MG, we have to accept the widespread existence of the NGRO in MG. Besides golden pentagon, golden rectangle and triangle are more easily to form in MG because they involve fewer atoms, which also can enhance the probability of NGRO appearing in MG to some degree. In fact, we not only propose the NGRO in our current work, but also have found some very important clues to confirm our conclusion from other literature.[20,34] For example, Khmich *et al.* calculated the ratio R_2/R_1 of $g(r)$ to be 1.64 in tantalum mono-atomic metallic glass,[20] and Liang *et al.* reported the ratio R_2/R_1 of $g(r)$ to be 1.69 for the $Mg_{70}Zn_{30}$ metallic glass.[34] Unfortunately, both of them did not calculate the value of R_1/R_2 in their papers. Obviously, R_1/R_2 is the reciprocal of R_2/R_1. When we use their raw data to calculate the value of R_1/R_2, we have surprisedly found that R_1/R_2 of $g(r)$ is equal to 0.6097 and 0.5917, respectively. The ratios of R_1/R_2 are consistent well with the ratio of P_1/P_2 (0.618) in our work. The existence of NGRO in metallic glass is confirmed indirectly and sufficiently in terms of the R_2/R_1 of $g(r)$ from different metallic glasses. Hence we further deduce that the NGRO is more universal compared to the LFFS in MG.

3.4. Electronic structure of Ta metallic glass

As early as in 1975, a nearly-free-electron model for explaining the relative stability of metallic glass was proposed by Nagel and Tauc.[37] Within the framework of the nearly-free-electron model, they have predicted that the maximum stability corresponds to the Fermi level (E_F) at a minimum of the density of states (DOS) in MG. Hence based on the above *ab-initio* simulations, in order to further understand the correlation between DOS and stability of metallic glass, we present a comparison of measured and calculated total density of states (TDOS) and partial density of states (PDOS) at four different temperatures (3800 K, 2500 K, 1800 K, and 300 K) in Fig. 9. From Fig. 9(a), one can see that the magnitude of 300 K is the minimum, and then 3800 K and 2500 K, followed by 1800 K at E_F. The result is consistent well with the nearly-free-electron model for explaining the relative stability of metallic glass,[37,38] and provides an obviously evidence for a minimum DOS at the Fermi level. From the insert of Fig. 9(a), it is found that TDOS mainly locates at −10 eV to 1 eV and obviously the DOS peak mainly locates at −7 eV to E_F. Meanwhile, the PDOS of the Ta system is also shown in Fig. 9(b). From Fig. 9(b), one can see that the DOS of d states is pushed to higher energies at the energetic range from −4 eV to 1 eV, and the kinetic energy is therefore greatly reduced, whereas the DOS mainly consists of s states when the energy is below −6.0 eV. The energetic range of coexistence of s, p, and d states is mainly located in −6.0 eV to −4.0 eV. In addition, compared to the liquid (3800 K) and super-cooled liquid (1800 K and 2500 K), figure 9(b) also shows that the deep energy state peak of DOS shifts clearly towards lower energies at 300 K, indicating that stronger s–s electronic interaction will induce shorter Ta–Ta bond. In fact, in 5d transition metals, the interactions between s electrons are known to contribute little to the reduction of the total electron energy.[39,40]

Next, to further understand the electronic interaction between different Ta atoms in the rapid solidification, the contour plots of difference electron densities on the sections cross the [110] and [011] planes ([110] and [011] refer specifically to the planes of the simulation box) in the liquid (3800 K) and amorphous solid (300 K) are illustrated in Fig. 10, respectively. At $T = 3800$ K, both of the contour plots of the [110]

and [011] planes show that the electric charge (denoted by blue color) originated from the parent atoms is enriched in different interatomic region, and the distribution is disorder. However, the phenomena have changed significantly in amorphous Ta at $T = 300$ K. From Fig. 10, one can see that the obviously orientation of covalent bond is presented in the [110] plane with layered and linear arrangement (denoted by the blank dashed line) of Ta atoms at $T = 300$ K. For the [011] plane at 300 K, the nonlinear covalent bond denoted by the path of dashed curve can be observed too. Thus a distinct anisotropic build-up of the directional covalent bonding charge in [110] plane at 300 K could be attributed to the NGRO with respect to the atomic arrangement in Ta metallic glass in Fig. 8.

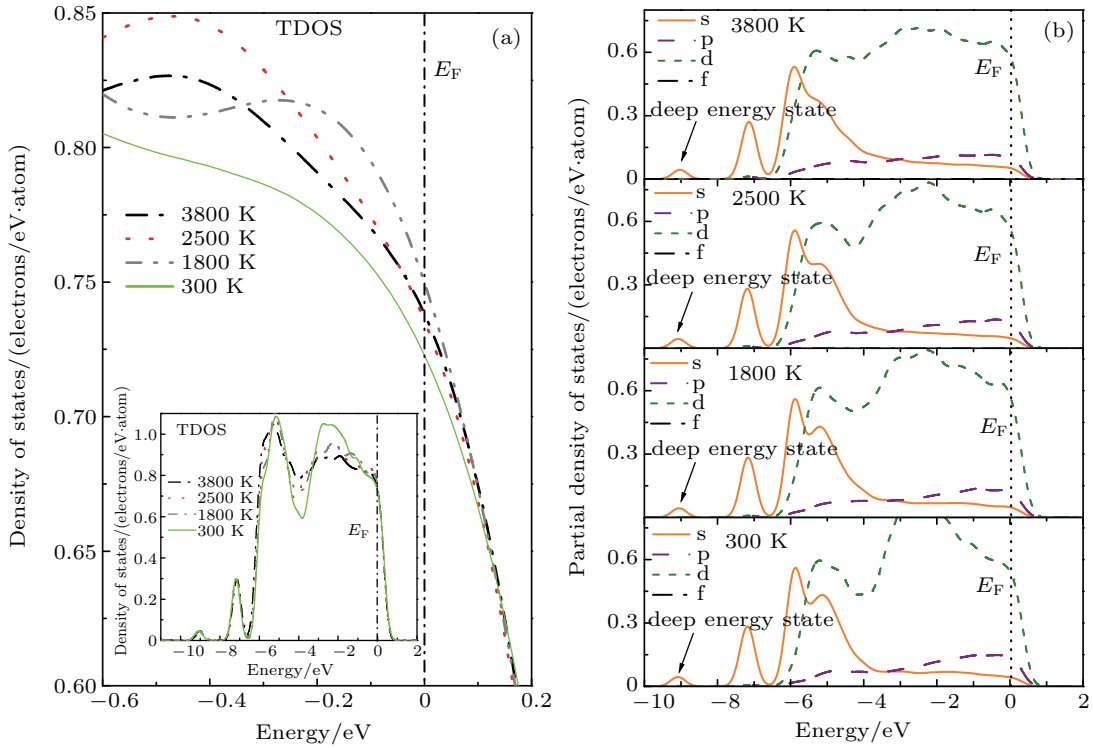

Fig. 9. (a) Total density of states (TDOS) and (b) partial density of states (PDOS) of the Ta system at deferent temperatures. The insert is the full view of TDOS. The Fermi levels E_F are indicated by the black dashed lines.

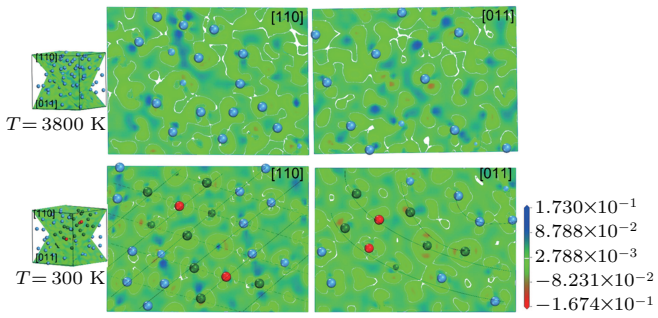

Fig. 10. Contour plots of difference electron densities on the sections cross the [110] and [011] planes of the simulated box in the liquid (3800 K) and amorphous solid (300 K) of Ta system. The red and green balls denote central and shell atoms of icosahedral clusters. The blue balls denote residual atoms in other local atomic configurations without the tracked icosahedra. The black dash lines are for guides to the eyes.

4. Discussion

Several commonly methods including of energy, atomic density, $g(r)$, microstructure analysis, bond lengths, density of states, and difference electron densities are used to illustrate the characteristics of structure for amorphous solid and supercooled liquid in this paper. Generally speaking, the variation of energy dependence of T is usually a key critical reference for determining the T_g during the rapid solidification. In this work, although only three different initial structure models are rapidly cooled perfectly as the computation time of DFT is very huge and consumed, and all of energy curves converge to be consistent at temperature below about 1750 K. But when $T > T_g$, the higher the temperature, the larger the difference in energy per atom, the more obvious the energetic fluctuation. This indicates that the super-cooled liquid has intrinsic variations and fluctuations and some important depth of information beyond our knowledge. Meanwhile, $T_g = 1750$ K is further confirmed by the temperature of splitting the second peak of the $g(r)$ curve. Although the origin of the split second peak for MGs has been the subject of some debate in recently years,[15] our microstructure analysis subsequently has revealed clearly that indeed original from ISRO and IMRO. Before further statistical analyzing the information of atomic distance and bond lengths between the nearest and second nearest neighbors in the system, we have used three standardized geometric diagrams (refer to Fig. 5) to explain strictly

why the golden ratio order is always hidden in these geometric structures from the perspective of mathematical logic. That is to say, if we admitted the existence of LFFS and icosahedral cluster in MGs system, it means that we have to admit the existence of golden section order. Excitedly, the existence of NGRO in the Ta metallic glass has been distinct confirmed by the probability density function of atomic distance in Figs. 7 and 8.

5. Conclusion

We have systematically investigated the formation of mono-atomic Ta metallic glass by using *ab-initio* MD calculations. A nearly golden ratio order is found from the distribution of probability density (P) as a function of the nearest and second-nearest atomic distances of ultrafast liquid Ta quenching processes. Although only limited examples have been studied, we believe that the NGRO is another universal structural feature in metallic glass besides LFFS. Analyzing of electronic structure shows that our results are consistent well with the nearly-free-electron model for explaining the relative stability of metallic glass. And the obviously orientation of covalent bond is presented in the [110] plane of the simulated box with linear arrangement of Ta atoms at $T = 300$ K, which could be attributed to the NGRO in Ta metallic glass.

Acknowledgment

We thank Dr. Shuang He for discussions and program compiling.

References

[1] Klement W, Willens R H and Duwez P 1960 *Nature* **187** 869
[2] Hirata A, Kang L J, Fujita T, *et al.* 2013 *Science* **341** 376
[3] Zeng Q S, Sheng H, Ding Y, *et al.* 2011 *Science* **332** 1404
[4] Cheng Y Q and Ma E 2011 *Prog. Mater. Sci.* **56** 379
[5] Lad K N and Jakse N 2012 *J. Chem. Phys.* **136** 104509
[6] Ding J, Cheng Y Q and Ma E 2014 *Acta Mater.* **69** 343
[7] Jiang Y Q, Peng P, Wen D D, *et al.* 2015 *Comput. Mater. Sci.* **99** 156
[8] Sheng H W, Luo W K, Alamgir F M, *et al.* 2006 *Nature* **439** 419
[9] Zhang Y, Zuo T T, Tang Z, *et al.* 2014 *Prog. Mater. Sci.* **61** 1
[10] Tong C J, Chen Y L, Chen S K, *et al.* 2005 *Metall. Materials Transactions A* **36** 881
[11] Singh S, Wanderka N, Murty B S, *et al.* 2011 *Acta Mater.* **59** 182
[12] Guo Y R, Qiao C, Wang J J, *et al.* 2019 *J. Alloys Compd.* **790** 675
[13] Yang Z J, Tang L and Wen T Q 2019 *J. Phys.: Condens. Matter* **31** 135701
[14] Tang L, Wen T Q and Wang N 2018 *Phys. Rev. Materials* **2** 033601
[15] Ding J, Ma E, Asta M, *et al.* 2015 *Sci. Rep.* **5** 17429
[16] Wen D D, Peng P, Jiang Y Q, *et al.* 2015 *J. Non-Cryst. Solids* **427** 199
[17] Wu Z Z, Mo Y F, Lang L, *et al.* 2018 *Phys. Chem. Chem. Phys.* **20** 28088
[18] Zhong L, Wang J W, Sheng H W, *et al.* 2014 *Nature* **512** 177
[19] Zhang J C, Chen C, Pei Q X, *et al.* 2015 *Mater. Des.* **77** 1
[20] Khmich A, Sbiaai K and Hasnaoui A 2019 *J. Non-Cryst. Solids* **510** 81
[21] Jiang D, Wen D D, Tian Z A, *et al.* 2016 *Physica A* **463** 174
[22] Yang M H, Li J H and Liu B X 2018 *J. Alloys Compd.* **757** 228
[23] Gangopadhyay A K and Kelton K F 2019 *J. Non-Cryst. Solids X* **2** 100016
[24] Kresse G and Hafner J 1993 *Phys. Rev. B* **47** 558
[25] Kresse G and Furthmuller J 1996 *Phys. Rev. B* **54** 11169
[26] Kresse G and Hafner J 1994 *J. Phys.:Condens. Matter* **6** 8245
[27] Kresse G and Joubert D 1999 *Phys. Rev. B* **59** 1758
[28] Monkhorst H J and Pack J D 1976 *Phys. Rev. B* **13** 5188
[29] Plimpton S 1995 *J. Comput. Phys.* **117** 1
[30] Martyna G J Tobias D J and Klein M L 1994 *J. Chem. Phys.* **101** 4177
[31] Cai J and Ye Y Y 1996 *Phys. Rev. B* **54** 8398
[32] Wen D D 2015 *A Simulation Study on the Heredity and Evolution of Clusters in Liquid Cu-Zr Alloys during the Rapid Solidication* (PhD Dissertation) (Changsha: Hunan University)
[33] Zhang Y, Mattern N and Eckert J 2012 *J. Appl. Phys.* **111** 053520
[34] Liang Y C, Liu R S, Mo Y F, *et al.* 2014 *J. Alloys Compd.* **597** 269
[35] Wendt H R and Abraham F F 1978 *Phys. Rev. Lett.* **41** 1244
[36] Peng H L, Li M Z and Wang W H 2011 *Phys. Rev. Lett.* **106** 135503
[37] Nagel S R and Tauc J 1975 *Phys. Rev. Lett.* **35** 380
[38] Moruzzi V L, Oelhafen P and Williams A R 1983 *Phys. Rev. B* **27** 7194
[39] Friedel J and Sayers C M 1977 *J. Phys.* **38** 697
[40] Friedel J 2001 *Adv. Phys.* **50** 539